Journal of Power Sources 209 (2012) 220–227

Contents lists available at SciVerse ScienceDirect

Journal of Power Sources

journal homepage: www.elsevier.com/locate/jpowsour

Diffusion induced stress in layered Li-ion battery electrode plates

Junqian Zhang[a,*], Bo Lu[b], Yicheng Song[a], Xiang Ji[b]

[a] Department of Mechanics and Shanghai Key Laboratory of Mechanics in Energy Engineering, Shanghai University, Shanghai 200444, China
[b] Shanghai Institute of Applied Mathematics and Mechanics, Shanghai University, Shanghai 200072, China

ARTICLE INFO

Article history:
Received 27 January 2012
Received in revised form 25 February 2012
Accepted 26 February 2012
Available online 5 March 2012

Keywords:
Lithium battery
Multilayer electrode
Current collector
Lithiation
Diffusion induced stress

ABSTRACT

In this paper, structural configuration of layered Li-ion battery electrode plates is evaluated by analytically formulating the diffusion induced stress. Both symmetric electrode and asymmetric bilayer electrode are discussed. The thickness ratio and the modulus ratio of current collector to active plate are analytically identified to be the important influence parameters on the stress. Applying a material with smaller elastic modulus for current collector could reduce the peak stresses in both current collector and active plate. Increasing the thickness of current collector would reduce the stress in itself while promote the stress in active plate. Therefore, from mechanical viewpoint on designing an electrode, the material for current collector should be as soft and flexible as possible. And the thickness of current collector should be in an appropriate range. Basically, it should be as small as possible on the precondition that the mechanical strength is satisfied. Finally, effects of three charging conditions, i.e. uniform, galvanostatic, and potentiostatic, on the diffusion induced stress is discussed. It is found the maximum stresses for three cases are linear to the total amount of intercalated lithium ions. Based on the stresses, an optimized charging operation, i.e. first galvanostatic followed by potentiostatic, is suggested.

1. Introduction

Internal stress in Li-ion battery electrode generated by intercalation and deintercalation of Li ions into and from active materials has received considerable attention because it is a direct cause of cracking which leads to the loss of capacity and the deterioration of cyclic performance. In the literature, the insertion/extraction of lithium ions and the induced stress in an electrode have often been modeled by using the continuum diffusion model coupled with continuum mechanics model. Some considered one-way coupling models where the diffusion is not affected by stress whereas the others adopted more sophisticated two-way coupling models where stress and diffusion are mutually affected. Huggins and Nix [1] presented a simple one-dimensional beam model for analysis of cracking caused by swelling transformation strain in bilayer plate structures. García et al. [2] performed a two dimensional numerical analysis of diffusion of Li-ions in both electrolyte and spherical active materials in cathode with results indicating that the large stresses develop during fast discharge. Christensen and Newman [3] developed a strongly coupled diffusion-stress model to calculate stress in spherical active particles emphasizing on the pressure-diffusion effect and the high Li-ions concentration. Zhang et al. [4] conducted one-dimensional modeling of a spherical active particles and three-dimensional simulations of ellipsoidal particles under galvanostatic Li ions intercalation; the numerical results for $LiMn_2O_4$ system suggest that particles with smaller sizes and larger aspect ratios lead to smaller intercalation-induced stresses. Cheng and Verbrugge [5] have developed analytical expressions for the evolution of stress and strain energy within a spherical particle under both galvanostatic and potentiostatic conditions. Using a diffusion-elasticity model with Butler–Volmer surface kinetics Golmon et al. [6] simulated the insertion of lithium into spherical silicon particles with results suggesting that the stresses depends strongly on the reaction kinetics and discharge rate. Using the cohesive model of crack Bhandakkar and Gao [7] predicted a critical characteristic dimension for crack nucleation in an initially crack-free strip electrode under galvanostatic intercalation and deintercalation processes. Qi and Harris [8] demonstrated graphically the lithium concentration spatial maps via the color variation in graphite and carried out an in situ observation of strain field during lithiation of a graphite electrode. Using the theory of diffusion-induced stress and the energy principle, Yang [9] derived an analytical relation between the critical concentration of solute atoms and average damage size for the insertion-induced cracking and buckling in an elastic film. Seo et al. [10] performed a finite element analysis of intercalation-induced stress in the $LiMn_2O_4$ particle with the surface morphology reconstructed using atomic force microscopy (AFM), showing that Mises stress at the sharply dented region is an order-of-magnitude higher than the stress in smooth particle. Zhao et al. [11] developed a coupled

* Corresponding author. Tel.: +86 21 6613 4972; fax: +86 21 6613 5258.
E-mail address: jqzhang2@shu.edu.cn (J. Zhang).

0378-7753/$ – see front matter © 2012 Elsevier B.V. All rights reserved.
doi:10.1016/j.jpowsour.2012.02.104

diffusion-large plastic deformation theory with application to analysis of the induced stress and plastic deformation in a spherical particle.

The most works mentioned above concerned the diffusion induced stress at particle level. Li diffusion and diffusion-induced stress at the higher scale of layered structure are usually neglected. It is very important to discuss the layered structural configuration where the multilayer electrode plate includes active plates as well as current collector. Furthermore, Li concentration gradient at the layer level in active plate during charging was experimentally observed [12], indicating that all active particles in the active plate are not charged simultaneously in some cases. The layered geometry is one of promising structural configurations for newly developed nanoelectrodes [13]. Therefore, focusing on the multilayer electrodes the purposes of this work are to: (1) introduce the spatial distribution of Li concentration and develop a general and yet analytical solution for diffusion-induced stress in multilayer electrode, (2) identify the parameters of layered structure which affect the diffusion-induced stress, (3) address the role of current collector on the induced stress in electrode.

2. Analysis

Consider an electrode plate in which two active material plates are bonded to a central current collector, Fig. 1, where h_1, h_2 and h_c denote the thickness of two active plates and current collector, respectively. The active plates are considered as composites containing both active particles and pore-filling electrolyte. Let the thickness direction be aligned with the z-axis and the in-plane of plate with x- and y-axes. Each individual layer in the electrode plate is assumed to be an isotropic and elastic material. Lithium ions are allowed to be inserted into and extracted out of the electrode plate from one side face of each active material plate, Fig. 1.

The diffusion of lithium ions in the thickness direction of electrode is assumed to be governed by Fick's law

$$\frac{\partial c}{\partial t} - D\frac{\partial^2 c}{\partial z^2} = 0 \tag{1}$$

where c is the molar concentration of lithium ion, D is the effective diffusivity of Li in the composite active material. It describes the macroscopic transportation process including diffusion and migration of lithium ions through the liquid phase, solid phase and the solid–liquid interfaces in the active plate. The initial solute concentration in the electrode is assumed to be zero, i.e.

$$c = 0 \quad \text{for } t = 0 \tag{2}$$

The boundary conditions for active Plate 1 in the electrode configuration shown in Fig. 1 are given by

$$D\frac{\partial c}{\partial z} = \frac{i_n}{F} \quad \text{for } z = h_1 \tag{3}$$

$$D\frac{\partial c}{\partial z} = 0 \quad \text{for } z = 0$$

for the galvanostatic charging, where i_n is the surface current density and $F = 96485.3\ \mathrm{C\,mol^{-1}}$ is Faraday's constant, and

$$c = c_0 \quad \text{for } z = h_1 \tag{4}$$

$$D\frac{\partial c}{\partial z} = 0 \quad \text{for } z = 0$$

for potentiostatic charging, where c_0 is the constant surface concentration. The solution for the ion concentration can be found as follows [14]

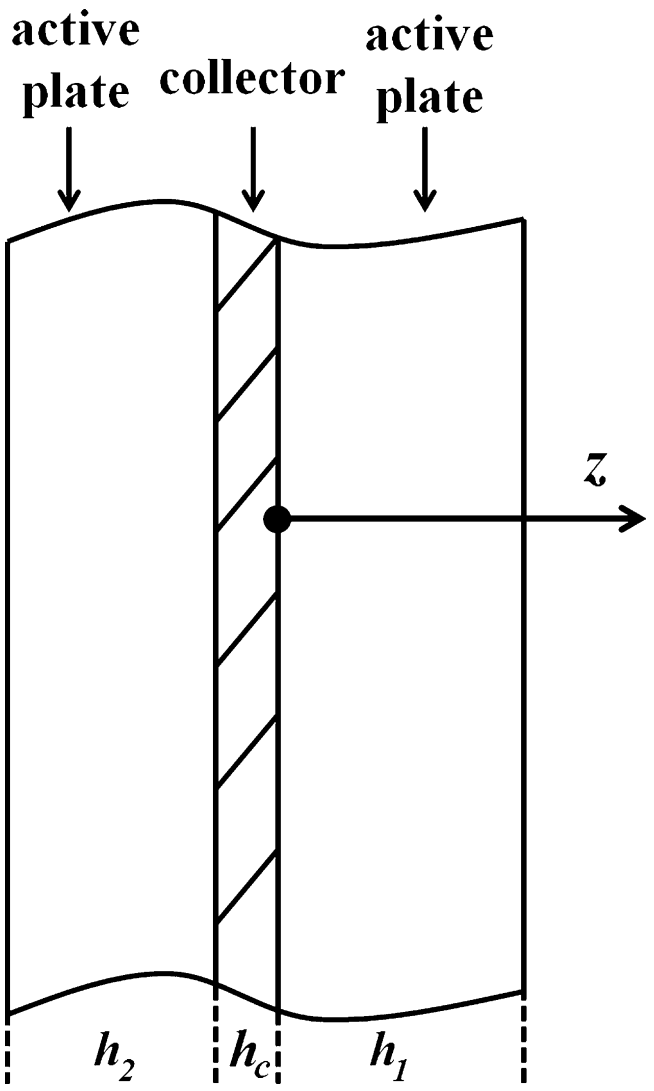

Fig. 1. Configuration of the electrode in which two active plates are bonded to the current collector. Here, $h_1 = h_2$ in symmetric electrode, while $h_1 \neq h_2$ in asymmetric case.

$$c(z,t) = \frac{i_n h_1}{FD}\left\{\frac{Dt}{{h_1}^2} + \frac{3z^2 - h_1^2}{6h_1^2} - \frac{2}{\pi^2}\sum_{n=1}^{\infty}\frac{(-1)^n}{n^2} \times \cos\frac{n\pi z}{h_1}\exp\left(-\frac{n^2\pi^2 Dt}{{h_1}^2}\right)\right\} \tag{5}$$

during galvanostatic charging, and

$$c(z,t) = c_0 - c_0\sum_{m=1}^{\infty}\frac{4(-1)^{m-1}}{(2m-1)\pi}\cos\left(\frac{(2m-1)\pi z}{2h_1}\right) \times \exp\left(-\frac{(2m-1)^2\pi^2 Dt}{4{h_1}^2}\right) \tag{6}$$

during potentiostatic charging. The concentration in the active Plate 2 can be obtained from above equations by replacing z-coordinate with $(-z–h_c)$.

The properties of active material such as Young's modulus could be significantly affected by the solute concentration [15]. Therefore, for generality here we assume that Young's modulus E, Poisson's

ratio ν and partial molar volume Ω depend upon the concentration, in turn, are implicit functions of z.

In large electrode plate the equal biaxial stress, $\sigma_{xx}(z)=\sigma_{yy}(z)$ which are functions of z only, is assumed to be generated by the inhomogeneous distribution of concentration given by Eq. (5) or (6). The other four stress components are zero. It is easy to verify that the equations of mechanical equilibrium, $\partial\sigma_{ji}/\partial x_j=0$, can be satisfied automatically. Furthermore, it is suggested that from the constitutive equations the two in-plane normal strain components are also equal, i.e. $\varepsilon_{xx}=\varepsilon_{yy}$. The six deformation compatibility equations lead to:

$$\frac{\partial^2\varepsilon_{xx}}{\partial z^2}=0 \tag{7}$$

This suggests that the in-plane normal strain varies linearly in thickness direction,

$$\varepsilon_{xx}=\varepsilon_{yy}=\varepsilon_0+z\kappa \tag{8}$$

where ε_0 is considered as in-plane strain at the plane of $z=0$ and κ is the curvature of deformed electrode. This suggests that the active plates and current collector plate have the same bending curvature when they are perfectly bonded. The constitutive equation for biaxial stress is

$$\sigma_{xx}=\sigma_{yy}=E'(\varepsilon_0+\kappa z)-\frac{1}{3}E'\Omega c \tag{9}$$

where $E'=E/(1-\nu)$ is the biaxial modulus, Ω is the partial molar volume of solute. The concentration related term $-E'\Omega c/3$ represents the diffusion induced stress, written in an analogue form of thermal expansion stress. This term should be removed for the current collector.

The traction-free boundary conditions on two side faces have been satisfied automatically. Since we focus on the diffusion induced stress which does not include the effect of external mechanical loading the end of plate is mechanically free and the mechanical boundary conditions could be specified as

$$\int_{-h_c-h_2}^{h_1}\sigma_{xx}\,dz=0 \tag{10}$$

$$\int_{-h_c-h_2}^{h_1}\sigma_{xx}z\,dz=0 \tag{11}$$

Substitution of Eq. (9) gives

$$\varepsilon_0\int_{-h_c-h_2}^{h_1}E'\,dz+\kappa\int_{-h_c-h_2}^{h_1}E'z\,dz=\frac{1}{3}\int_{-h_c-h_2}^{h_1}E'\Omega c\,dz \tag{12}$$

$$\varepsilon_0\int_{-h_c-h_2}^{h_1}E'z\,dz+\kappa\int_{-h_c-h_2}^{h_1}E'z^2\,dz=\frac{1}{3}\int_{-h_c-h_2}^{h_1}E'\Omega cz\,dz \tag{13}$$

Solving for ε_0 and κ leads to

$$\varepsilon_0=\frac{IN^c-BM^c}{AI-B^2} \tag{14}$$

$$\kappa=\frac{AM^c-BN^c}{AI-B^2} \tag{15}$$

where A, B and I are biaxial extensional stiffness, biaxial stretching–bending coupling stiffness and biaxial bending stiffness, N^c and M^c are concentration force resultant and concentration moment resultant, given by

$$A=\int_{-h_c-h_2}^{h_1}E'\,dz,\qquad B=\int_{-h_c-h_2}^{h_1}E'z\,dz,\qquad I=\int_{-h_c-h_2}^{h_1}E'z^2\,dz$$
$$N^c=\frac{1}{3}\int_{-h_c-h_2}^{h_1}E'\Omega c\,dz,\qquad M^c=\frac{1}{3}\int_{-h_c-h_2}^{h_1}E'\Omega cz\,dz \tag{16a-e}$$

Here we emphasize that the above obtained solutions for stress and strain are exact because all mechanical field equations of three-dimensional elasticity, interface continuity conditions and boundary conditions have been satisfied.

3. Symmetric electrode plates

In this section we exam the electrode which includes two active material plates with equal thickness by setting $h_2=h_1$. The active material is assumed to expand isotropically upon charging. The battery is assumed to be under galvanostatic operation. Considering a battery in which the cathode and anode are placed face to face, lithium ions are inserted into electrode firstly from both side faces. If the effect of concentration on the material properties is neglected the biaxial modulus and partial molar volume of active plate, E_1' and Ω, and the biaxial modulus of current collector, E_c', then, are constant and independent of z-coordinate. It follows from Eqs. (14)–(16) that

$$A=E_1'h_1\left(2+\frac{h_c}{h_1}\frac{E_c'}{E_1'}\right),\qquad B=-\frac{1}{2}E_1'h_ch_1\left(2+\frac{h_c}{h_1}\frac{E_c'}{E_1'}\right)$$
$$I=E_1'{h_1}^3\left(\frac{2}{3}+\frac{h_c}{h_1}+\left(\frac{h_c}{h_1}\right)^2+\frac{1}{3}\left(\frac{h_c}{h_1}\right)^3\frac{E_c'}{E_1'}\right)$$
$$N^c=\frac{2}{3}E_1'\Omega\int_0^{h_1}c(z)\,dz,\qquad M^c=-\frac{1}{3}E_1'\Omega h_c\int_0^{h_1}c(z)\,dz \tag{17a-e}$$

$$\kappa=0 \tag{18}$$

$$\varepsilon_0=\frac{2}{3}\left(\frac{1}{2+(h_c/h_1)(E_c'/E_1')}\right)\frac{\Omega}{h_1}\int_0^{h_1}c(z)\,dz \tag{19}$$

The closed-form expressions for the equal biaxial stress in the active plates and current collector can be obtained,

$$\sigma_1(z,t)=\frac{i_nE_1'\Omega h_1}{3FD}\left[-\chi\bar{t}+\frac{1}{6}-\frac{1}{2}\bar{z}^2+\frac{2}{\pi^2}\sum_{n=1}^{\infty}\frac{(-1)^n}{n^2}\times\cos(n\pi\bar{z})\exp(-n^2\pi^2\bar{t})\right] \tag{20}$$

$$\sigma_c(z,t)=\frac{i_nE_c'\Omega h_1}{3FD}(1-\chi)\bar{t} \tag{21}$$

where $\bar{t}=\frac{Dt}{h_1^2}$, $\bar{z}=\frac{z}{h_1}$, $\chi=(h_c/h_1)(E_c'/E_1')/(2+(h_c/h_1)(E_c'/E_1'))$

The interesting is that the stress in the current collector in the electrode does not vary along the thickness direction. This is because the plate curvature κ is equal to zero in the large and symmetric layered electrode structure. The biaxial stress in the current collector, expressed in Eq. (9), is thus irrelevant with the coordinate z in the thickness direction.

Fig. 2 shows the distribution of lithium ions concentration along thickness. As lithium ions continuously go into the active plate, the lithiated region tends to expand, while the unlithiated region and the current collector tend to remain undeformed. Therefore, compressive stress is generated in the active plates due to the restriction from the current collector, while tensile stress is caused in the current collector because of the traction of active plates. Both stresses keep increasing as more and more lithium ions migrate into the active plates, as illustrated in Fig. 3. In the calculation, the current collector is considered as copper, and the active plate is assumed to be graphite plate. Therefore, the modulus ratio of the two layers E_c'/E_1' is chosen to be 10. The thickness ratio of the two layers h_c/h_1 is 0.25, determined from experimental observation [12].

It can be concluded from Figs. 2 and 3 that the stress in a large active plate under galvanostatic charging mainly depends

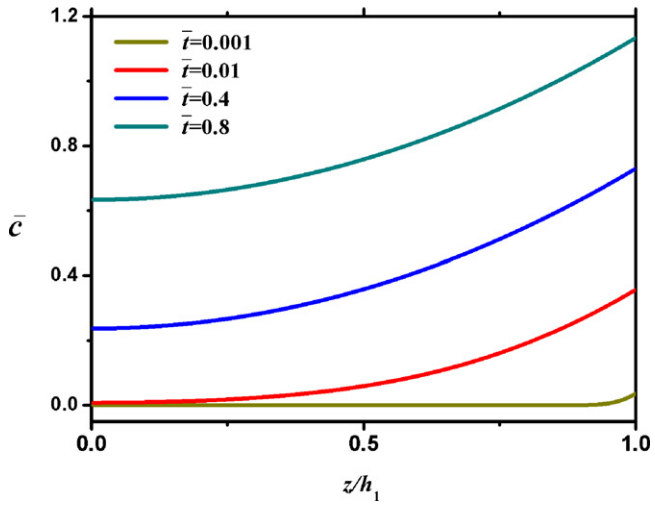

Fig. 2. Dimensionless lithium ions concentration $\bar{c}$ ($\bar{c} = cFD/i_n h_1$) along the plate thickness under galvanostatic charging. Here, $z/h_1 = 0$ represents the interface between the current collector and active plate, $z/h_1 = 1$ represents the side face of active plate.

on Li concentration. The region with higher Li concentration corresponds to a larger stress level. Therefore, the maximum stress in the active plate is found to be at the side face where lithium ions firstly migrate into the active plate.

One of the main purposes of this work is to discuss the parameters of layered structure which affect the diffusion induced stress. Here are two important parameters from mechanics viewpoint, i.e. the modulus ratio of current collector to active plate as well as the thickness ratio of the two layers.

Fig. 4 shows the variation of biaxial stress along the whole electrode thickness with respect to different modulus ratio E_c'/E_1'. It clearly shows that both the tensile stress in current collector and the compressive stress in the active plate reduce as the ratio E_c'/E_1' declines, but more remarkably in the current collector. This phenomenon suggests that a softer and more flexible current collector would help to reduce the restriction between the two layers, and thereby reducing the stress in the whole electrode. Soft material is thus preferred in the material selection in designing of current

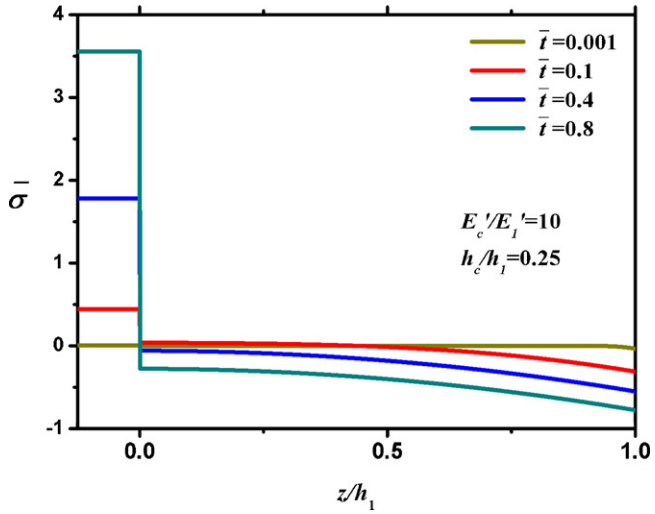

Fig. 3. The normalized biaxial stress $\bar{\sigma}$ ($\bar{\sigma} = \sigma_1/(E_1' \Omega i_n h_1/3FD)$ in the active plate, and $\bar{\sigma} = \sigma_c/(E_1' \Omega i_n h_1/3FD)$ in the current collector) along the electrode thickness under galvanostatic charging. Here, $z/h_1 < 0$ represents the region in the current collector, $z/h_1 > 0$ represents the region in the active plate.

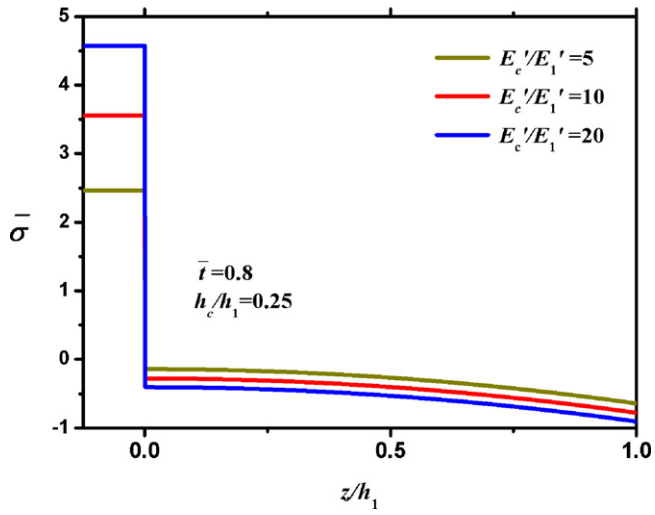

Fig. 4. Variation of the normalized biaxial stress $\bar{\sigma}$ along thickness with different modulus ratio E_c/E_1 in both current collector and active plate.

collector on the condition that the electrochemical properties are satisfied.

Regarding the geometrical configuration, Figs. 5 and 6 show the stress in the current collector and the active plate with respect to different thickness ratio h_c/h_1, respectively. As shown in Fig. 5, the layered structure electrodes with larger thickness ratio h_c/h_1 result in much smaller stress in the current collector during charging. Especially, at dimensionless charging time $\bar{t} = 0.8$, the stress in current collector is reduced much more than half. Therefore, a larger thickness ratio is beneficial to the strength of current collector.

However, thicker current collector means stronger restriction to the active plate. Thinner current collector could elongate more during charging, to some extent enabling the active plate more relaxed. As shown in Fig. 6, thicker current collector induces larger stress in the active plate. If it was in discharging, the thicker current collector would induce larger tensile stress which is critical to mechanical failure such as debonding and fracture.

Therefore, considering the strength of both current collector and active plate, the thickness ratio h_c/h_1 could not be too small for safety of current collector, neither could it be too large in order to decrease the stress in the active plate and provide enough rooms for the active materials. From mechanical viewpoint, the current

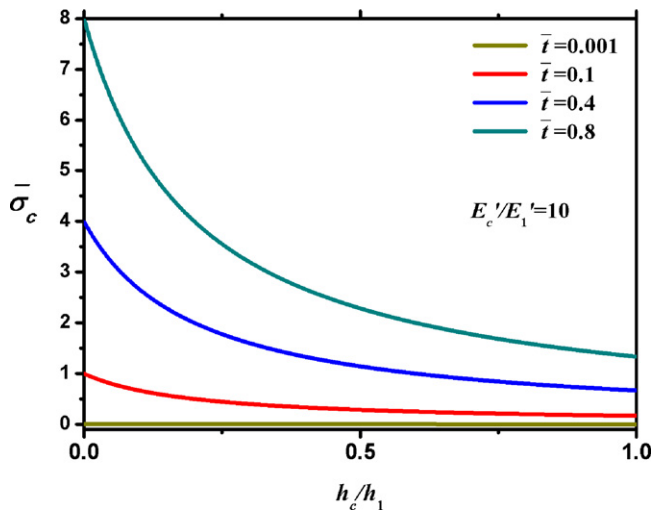

Fig. 5. Variation of the normalized biaxial stress $\bar{\sigma}_c$ ($\bar{\sigma}_c = \sigma_c/(E_1' \Omega i_n h_1/3FD)$) in the current collector with respect to the ratio of h_c/h_1 under galvanostatic charging.

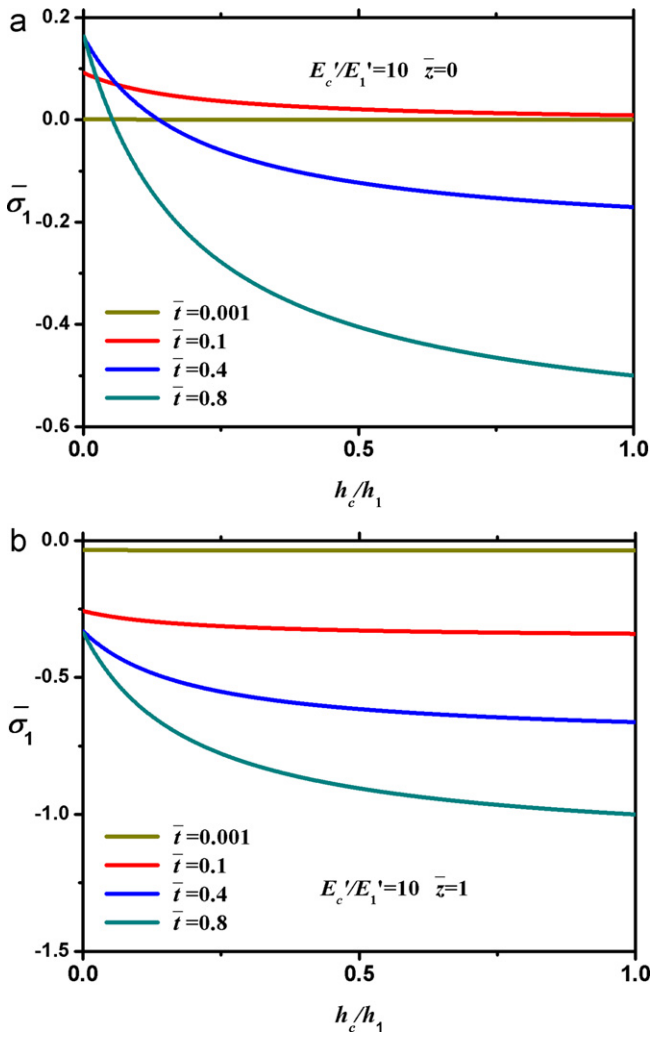

Fig. 6. Variation of the normalized biaxial stress $\bar{\sigma}_1$ ($\bar{\sigma}_1 = \sigma_1/(E_1'\Omega i_n h_1/3FD)$) in the active plate with respect to the ratio of h_c/h_1 under galvanostatic charging: (a) at the interface between current collector and active plate, $z/h_1 = 0$; (b) at the side face of the active plate, $z/h_1 = 1$.

collector should be as thin as possible on the precondition that the strength is satisfied.

4. Bilayer electrode plate

Here we exam the bilayer electrodes where a single active plate is bonded to current collector. By substituting $h_2 = 0$ into the solution derived in Section 2 we have the expressions for the curvature and the stresses in the active layer and current collector as follows,

$$\kappa = \frac{i_n\Omega}{FD}\left\{\beta_1\bar{t} + \beta_2\left\{\frac{1}{24} - \frac{2}{\pi^4}\sum_{n=1}^{\infty}\frac{(1+(-1)^{n+1})}{n^4}\exp(-n^2\pi^2\bar{t})\right\}\right\} \quad (22)$$

$$\sigma_1(z,t) = \frac{i_n E_1'\Omega h_1}{3FD}\left\{(\alpha_1 + 3\beta_1 z - 1)\bar{t} - \frac{3\bar{z}^2-1}{6} + \frac{2}{\pi^2}\sum_{n=1}^{\infty}\frac{(-1)^n}{n^2}\cos(n\pi\bar{z})\exp(-n^2\pi^2\bar{t})\right\}$$
$$+ \frac{i_n E_1'\Omega h_1}{3FD}(\alpha_2 + 3\beta_2\bar{z})\left\{\frac{1}{24} - \frac{2}{\pi^4}\sum_{n=1}^{\infty}\frac{(1+(-1)^{n+1})}{n^4}\exp(-n^2\pi^2\bar{t})\right\} \quad (23)$$

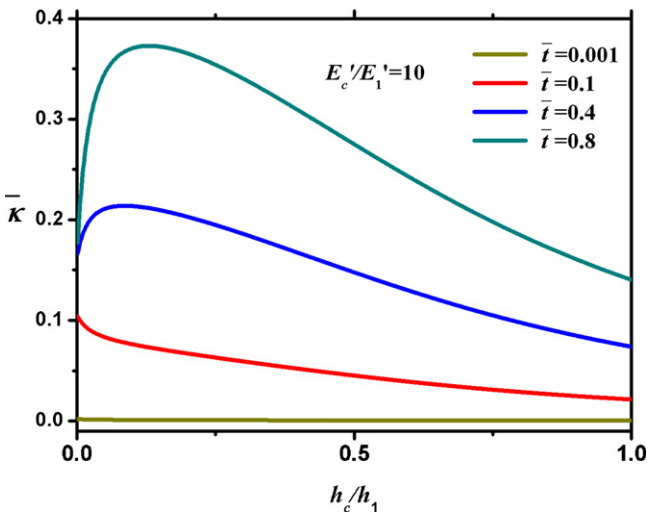

Fig. 7. Variation of dimensionless plate curvature $\bar{\kappa}$ ($\bar{\kappa} = \kappa FD/i_n\Omega$) at different charging time with respect to the thickness ratio h_c/h_1 in bilayer electrode.

$$\sigma_c(z,t) = \frac{i_n E_c'\Omega h_1}{3FD}\left\{(\alpha_1 + 3\beta_1\bar{z})\bar{t} + (\alpha_2 + 3\beta_2\bar{z}) \times \left[\frac{1}{24} - \frac{2}{\pi^4}\sum_{n=1}^{\infty}\frac{(1+(-1)^{n+1})}{n^4}\exp(-n^2\pi^2\bar{t})\right]\right\} \quad (24)$$

where

$$\alpha_1 = \frac{1}{\alpha_3}\left[7 + 3\frac{E_c'}{E_1'}\left(\frac{h_c}{h_1}\right)^2 + 4\frac{E_c'}{E_1'}\left(\frac{h_c}{h_1}\right)^3\right], \qquad \alpha_2 = \frac{6}{\alpha_3}\left[1 + \frac{E_c'}{E_1'}\left(\frac{h_c}{h_1}\right)^2\right]$$
$$\alpha_3 = 1 + 4\frac{E_c'}{E_1'}\frac{h_c}{h_1} + 6\frac{E_c'}{E_1'}\left(\frac{h_c}{h_1}\right)^2 + 4\frac{E_c'}{E_1'}\left(\frac{h_c}{h_1}\right)^3 + \left(\frac{E_c'}{E_1'}\right)^2\left(\frac{h_c}{h_1}\right)^4$$
$$\beta_1 = \frac{2}{\alpha_3}\frac{E_c'}{E_1'}\frac{h_c}{h_1}\left(1 + \frac{h_c}{h_1}\right), \qquad \beta_2 = \frac{4}{\alpha_3}\left(1 + \frac{E_c'}{E_1'}\frac{h_c}{h_1}\right)$$

In bilayer electrode, the most important feature is that the curvature $\kappa \neq 0$. As result, not only diffusion induced stress, but also bending stress will evolve during charging.

In bilayer electrode, the charging process is the same as that in symmetric electrode. Fig. 7 shows the effects of thickness ratio h_c/h_1 on electrode plate curvature. When there is no current collector ($h_c/h_1 = 0$), the curvature is not so large. The deformation of the active plate is purely determined by Li intercalation. Once a thin current collector is attached, the restriction will inhibit the expansion of the active plate in the region adjacent to the interface, and thereby increase the curvature. Once a thicker current collector is attached, because the current collector usually possesses much higher modulus, its large flexural rigidity becomes more dominant, and thus reduces the overall curvature of the electrode. This is the reason why the curvature κ is found to be firstly promoted, and then reduced with respect to the increase of h_c/h_1 in Fig. 7.

Fig. 8 shows the dimensionless biaxial stress during charging in both layers. It is found that both layers subject to compressive and tensile stress simultaneously. Generally, in the active plate, compressive stress is induced near the interface because the lithiation

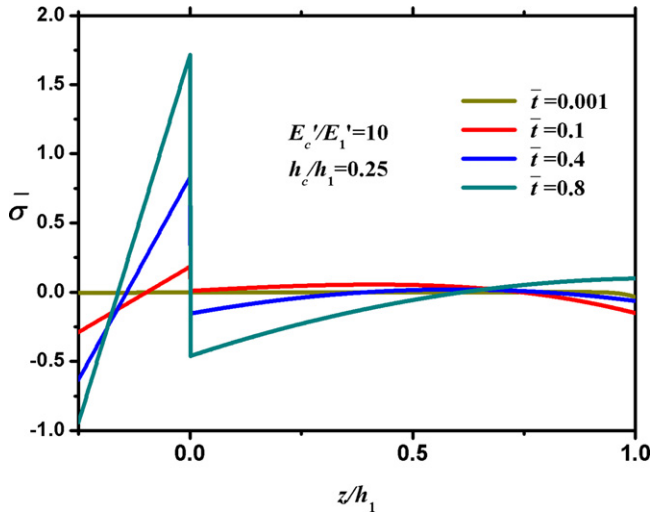

Fig. 8. The normalized biaxial stress $\bar{\sigma}$ along thickness at different time under galvanostatic charging. Here, $z/h_1 < 0$ represents the region in the current collector, $z/h_1 > 0$ represents the region in the active plate.

induced expansion is restricted by current collector. While in the region near the side face the stress changes from compressive to tensile as charging goes on. This is the result of competition between diffusion induced stress and bending stress. At beginning of lithiation, the curvature is small. The overall stress is mainly determined by diffusion induced stress. As more and more lithium ions migrate into the active plate, the curvature increases dramatically, resulting in a convex curvature at the side face. And thus, the stress near the side face changes to tensile because bending becomes more important.

Once certain amount of Li has been intercalated, the peak stress in both layers is found at the interface. It suggests that considerably large stress near the interface is essential to make the deformation compatible. Since the large peak stress is very important to structural failure, such as fracture, here is a key question: how to reduce the interaction between layers, and thus reduce the stress in electrode by modifying the electrode structure?

Part of the answer can be found in Fig. 9, which shows the biaxial stress in the current collector at the interface upon charging. The stress is found to decrease dramatically with increasing of current collector thickness when the ratio h_c/h_1 is not so large. This

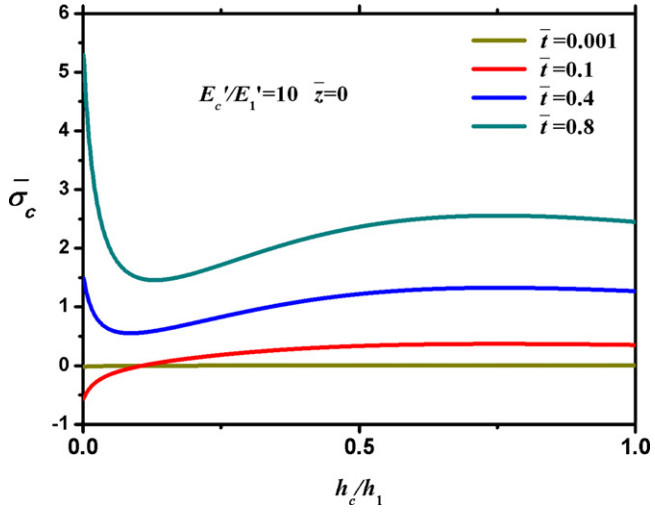

Fig. 9. Variation of the normalized biaxial stress $\bar{\sigma}_c$ at the interface in the current collector side with respect to the ratio of h_c/h_1 under galvanostatic charging.

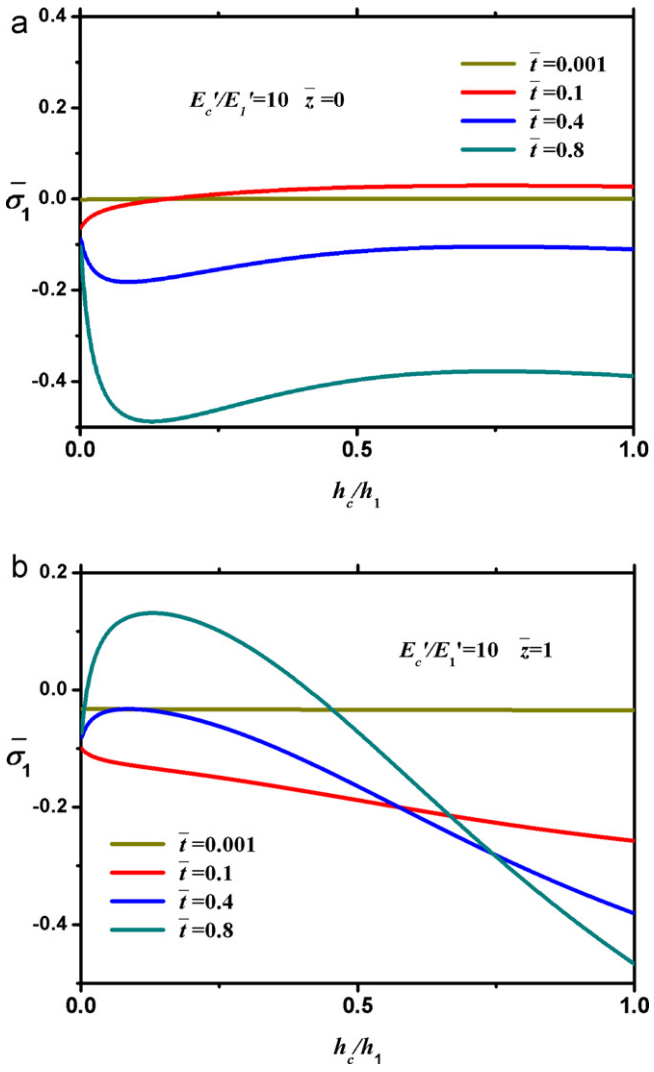

Fig. 10. Variation of the normalized biaxial stress $\bar{\sigma}_1$ in the active plate with respect to different ratio of h_c/h_1 under galvanostatic charging: (a) at the interface between current collector and active plate, $z/h_1 = 0$; (b) at the side face of the active plate, $z/h_1 = 1$.

decrease may be attributed to the increase of cross section area. However, when the ratio h_c/h_1 increases continuously, the stress is found to go up again. This may be attributed to the decrease of electrode curvature κ, as shown in Fig. 7. When the ratio h_c/h_1 increases from around 0.1, the deformation of current collector changes from bending-dominant to elongating-dominant, and thus slightly increases the biaxial stress. On the whole, increasing the thickness ratio h_c/h_1 could help to reduce the biaxial stress in the current collector.

Fig. 10 shows the biaxial stress in the active plate with respect to different thickness ratio h_c/h_1 upon charging, at both the interface ($\bar{z} = 0$) and side face ($\bar{z} = 1$). Unfortunately, it is found that increasing of thickness ratio h_c/h_1 would increase the peaks stresses, no matter compressive or tensile. This is very easy to understand if we draw an analogy to thermal expansion. It is the restriction of thermal expansion, not the expansion itself, induces thermal stress. Here, increasing of thickness ratio represents stronger restriction. Therefore, the stresses are found to be promoted with thicker current collector. Again, a similar conclusion to that in the symmetric case can be drawn that the current collector should be as thin as possible.

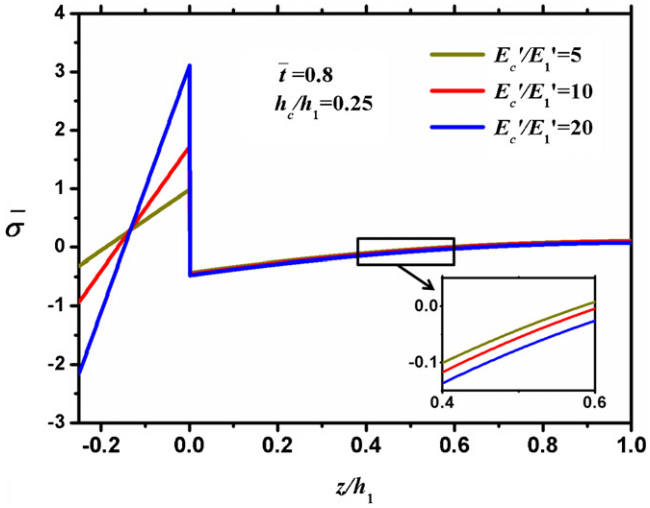

Fig. 11. Variation of the normalized biaxial stress $\bar{\sigma}$ along electrode thickness with different modulus ratio E_c/E_1 in the bilayer electrode.

The peak stress can be relaxed by modifying the material's elastic property. Fig. 11 shows that stress in the current collector is greatly reduced by decreasing the ratio of elastic modulus of current collector to active plate, i.e. E_c'/E_1'. It suggests that application of appropriate material for current collector could help to reduce the stress in both layers. As discussed above, a softer and more flexible current collector imposes less restriction to the active plate, and therefore reduces the stress in both layers. In the calculation shown in Fig. 11, the current collector is thin compared with the active plate. The ratio is only 1:4. Therefore, the stress reduction is very obvious in current collector, but not so evident in active plate.

5. Charging conditions

Another purpose of this work is to address the effects of charging conditions. In literature, most works implicitly assume that lithium ions migrate into all active particles at the same time because all particles are soaked in electrolyte. However, due to the limited porosity in electrode as well as the limited diffusion velocity of lithium ions in electrolyte, it is very difficult for all active particles to react with lithium ions simultaneously. In experiment, Li concentration gradient in active plate during charging has been observed [12]. It is necessary to investigate the effects of different charging conditions.

Influence of three charging conditions, i.e. uniform, galvanostatic and potentiostatic, on the stress in active plate are to be discussed. Due to the different charging duration, it is very difficult to compare the three charging process with respect to Newtonian time. It would be better to take the total amount of intercalated lithium ions as the scale of charging process. Furthermore, it will be revealed from following derivation that the expressions for the stresses in terms of the total amount ions are much simpler than that in terms of Newtonian time.

For simplicity, the symmetric electrode layered structure is considered. The influence of plate curvature is thus excluded. Write the dimensionless total amount of intercalated lithium ions as

$$\bar{Q} = \frac{FD}{i_n h_1^2} \int_0^{h_1} c(z)\, dz \tag{25}$$

The stress during uniform charging can be obtained from Eq. (9):

$$\sigma_{u,\max} = \frac{\sigma_1}{E_1' \Omega i_n h_1 / 3FD} = -\chi \bar{Q} \tag{26}$$

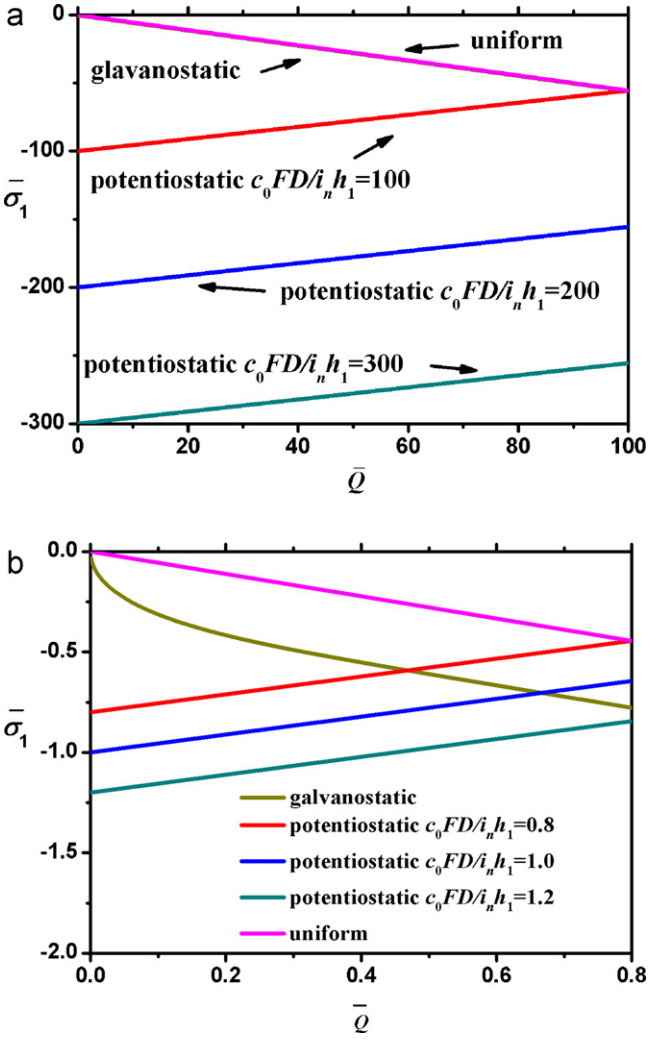

Fig. 12. The maximum diffusion induced stresses $\bar{\sigma}_1$ with respect to dimensionless total amount of intercalated lithium ions in three charging conditions: (a) overview in which the potentiostatic case is plotted with different ratio of c_0FD/i_nh_1; (b) enlarged view to show the intersection of stress lines corresponding to different charging conditions.

According to Fig. 3, the maximum stress in non-uniform charging is found at the side face where $\bar{z} = 1$. Combining Eq. (25) with Eqs. (20) and (23), the maximum stress can be obtained

$$\sigma_{g,\max} = \frac{\sigma_1(1,\bar{Q})}{E_1' \Omega i_n h_1 / 3FD}$$

$$= -\chi \bar{Q} - \frac{1}{3} + \frac{2}{\pi^2} \sum_{n=1}^{\infty} \frac{1}{n^2} \exp\left(-n^2 \pi^2 \bar{Q}\right) \tag{27}$$

for galvanostatic charging, and

$$\sigma_{p,\max} = \frac{\sigma_1(1,\bar{Q})}{E_1' \Omega i_n h_1 / 3FD} = -\chi \bar{Q} + \bar{Q} - \frac{c_0 FD}{i_n h_1} \tag{28}$$

for potentiostatic charging. Although the expressions of stress in terms of Newtonian time is very complicated, it is of interesting that they are very simple here. The stress in uniform and potentiostatic charging is exactly linear to the dimensionless total amount of intercalated lithium ions $\bar{Q}$. And in galvanostatic case with sufficient charging, the stress is also linear to $\bar{Q}$ with expression

$$\frac{\sigma_1(1,\bar{Q})}{E_1' \Omega i_n h_1 / 3FD} = -\chi \bar{Q} - \frac{1}{3} \tag{29}$$

since the progression term approaches to zero.

Fig. 12, which plots the stresses against the dimensionless total amount of intercalated lithium ions, reveals very important features of the maximum diffusion induced stress in the whole charging history with respect to three kinds of conditions. Generally, the maximum stress in potentiostatic charging $\sigma_{p,max}$ is always larger than that in uniform case $\sigma_{u,max}$ during whole duration except the last minute when the electrode is saturated and $\sigma_{p,max} = \sigma_{u,max}$.

Comparing uniform and galvanostatic charging, Fig. 12 shows that the stress lines of the two stresses become parallel after sufficient charging with a dimensionless difference of 1/3. This can also be verified with Eqs. (26) and (29). The progression term in Eq. (27) only makes effects in the early stage of charging.

Comparing potentiostatic and galvanostatic cases, it is found that there is a cross point of the stress lines corresponding to the two charging conditions. Combining Eqs. (27) and (29), the cross point is at $\bar{Q} = c_0 FD/i_n h_1 - 1/3$. It means that $\sigma_{p,max} > \sigma_{g,max}$ when $\bar{Q}$ is smaller than the critical value, vice verse, $\sigma_{p,max} < \sigma_{g,max}$ when $\bar{Q}$ is larger than the critical value. This suggests an optimized charging operation to reduce the diffusion induced stress, i.e. first galvanostatic charging followed by potentiostatic.

On the whole, the maximum stress in potentiostatic charging is far larger than the other two cases in almost whole charging history. The maximum stress in galvanostatic charging is larger than that in uniform case with a dimensionless value of 1/3, except the beginning stage. Our results show that effects of Li concentration gradient on stress in composite level cannot be neglected. Calculation based on uniform charging would result in smaller peak stress, and in turn, gives an overestimation on electrode strength.

6. Concluding remarks

In this paper, layered structures applied in lithium ion batteries have been evaluated by formulating the diffusion induced stress. The mechanical role of current collector has been addressed. Finally, different charging conditions are compared and discussed.

In an electrode where the active material expands upon lithiation, current collector acts as substrate of active plate. It restricts the expansion of active plate, and also deforms with the plate. In a large electrode with symmetric layered structure, current collector and active plates are elongated without bending. Current collector is subjected to uniform tensile stress. The active plates are subjected to non-uniform compressive stress which heavily depends on the distribution of Li concentration. The peak stress in the active plate is found at the side faces where lithium ions firstly migrate into the plate. While in a large electrode with asymmetric bilayer structure, both elongation and bending are found during lithiation. Current collector is subjected to non-uniform stress caused by bending. Stress in the active plate is sum of bending stress and diffusion induced stress. And the peak stress is found at the interface. From viewpoint of mechanical role, thicker current collector could help to reduce the stress in itself while increase the stress in active plate. Therefore, current collector should be as thin as possible based on the precondition that strength is satisfied. It is also found the current collector with smaller elastic modulus would result in much lower stress in electrode. It suggests an effective way to release the stress in electrode, i.e. choosing softer and more flexible material for current collector. Finally, effects of three charging conditions, i.e. uniform, galvanostatic, and potentiostatic, on the diffusion induced stress is discussed. It is found the maximum stresses for three cases are linear to the total amount of intercalated lithium ions. The maximum stress in potentiostatic charging is far larger than the other two cases in almost whole charging history. The maximum stress in galvanostatic charging is larger than that in uniform case with a dimensionless value of 1/3, except the beginning stage. Based on the stresses, an optimized charging operation, i.e. first galvanostatic followed by potentiostatic, is suggested.

Acknowledgements

The authors gratefully acknowledge the financial supports by the National Science Foundation of China under Grant numbers 11172159, 11102103 and 11072137, as well as the Shanghai Leading Academic Discipline Project under project number S30106.

References

[1] R.A. Huggins, W.D. Nix, Ionics 6 (2000) 57–63.
[2] R.E. García, Y.M. Chiang, W.C. Carter, P. Limthongkul, C.M. Bishop, J. Electrochem. Soc. 152 (2005) A255–A263.
[3] J. Christensen, J. Newman, J. Solid State Electron. 10 (2006) 293–319.
[4] X. Zhang, W. Shyy, A.M. Sastry, J. Electrochem. Soc. 154 (2007) A910–A916.
[5] Y.T. Cheng, M.W. Verbrugge, J. Power Sources 190 (2009) 453–460.
[6] S. Golmon, K. Maute, S.H. Lee, M.L. Dunn, Appl. Phys. Lett. 97 (2010) 033111.
[7] T.K. Bhandakkar, H.J. Gao, Inter. J. Solids Struct. 47 (2010) 1424–1434.
[8] Y. Qi, S.J. Harris, J. Electrochem. Soc. 157 (2010) A741–A747.
[9] F. Yang, J. Power Sources 196 (2011) 465–469.
[10] J.H. Seo, M. Chung, M. Park, S.W. Han, X.C. Zhang, A.M. Sastry, J. Electrochem. Soc. 158 (2011) A434–A442.
[11] K.J. Zhao, M. Pharr, S.Q. Cai, J.J. Vlassak, Z.G. Suo, J. Am. Ceram. Soc. 94 (2011) S226–S235.
[12] S.J. Harris, A. Timmons, D.R. Baker, C. Monroe, Chem. Phys. Lett. 485 (2010) 265–274.
[13] A. Mukhopadhyay, A. Tokranov, K. Sena, X.C. Xiao, B.W. Sheldon, Carbon 49 (2011) 2742–2749.
[14] J. Crank, The Mathematics of Diffusion, Oxford University Press, 1979.
[15] R. Deshpande, Y. Qi, Y.T. Cheng, J. Electrochem. Soc. 157 (2010) A967–A971.